

Sources of light particles in peripheral collisions

P.L. Gonthier, J.D. Lenters, M.T. Vonk, D. Bleitz, and T. Koppenol
Department of Physics, Hope College, Holland, Michigan 49423

D.A. Cebra, W.K. Wilson, A. Vander Molen, J. Karn, S. Howden, A. Nadasen,*
 J.S. Winfield, and G.D. Westfall
*Michigan State University,
 National Superconducting Cyclotron Laboratory and
 Department of Physics and Astronomy,
 East Lansing, Michigan 48824*
 (Received 13 June 1990)

By studying light charged particles emitted in coincidence with projectile-like fragments, we probe heavy ion reaction mechanisms that result in the production of light particles in peripheral collisions. Triple coincidence α - α - ^{12}C correlations in the reactions of 35 MeV/nucleon ^{16}O with Ni conclusively identify previously known sources of light particles. The fast, beam velocity component of α particles in coincidence with projectile-like fragments is associated with the breakup of the projectile. The correlations suggest that the origin of the intermediate velocity component of α particles is the target nucleus. Both of these components are characterized by α particles emitted during the early stages of the collision.

Extensive studies¹⁻²³ of correlations between light particles and projectile-like fragments in heavy ion reactions indicate that a significant yield of projectile-like fragments is accompanied by the production of light particles focused in the beam direction with velocities approaching the velocity of the beam. The emission of light particles in such peripheral collisions has been associated with various production mechanisms such as the formation of hot spots,^{1,7} Fermi jets,⁸ piston effect,⁹ quasifree knockout,¹⁰ and projectile breakup.^{11,12} In such mechanisms emission is expected to take place during the early stages of the collision, thereby providing a probe of the reaction mechanism that yields information on the dissipation of the energy during the collision. However, the projectile and target nuclei can be excited to particle unbound states that are long lived. Decay of such states leads to sequential processes. Sequential emission is the decay of statistically equilibrated projectile-like fragments (PLF's), defined here as fragments with $Z_{\text{PLF}} \approx Z_{\text{projectile}}$, and target-like fragments (TLF's), defined here as fragments with $Z_{\text{TLF}} \approx Z_{\text{target}}$, that have been fully accelerated by the Coulomb field of the two interacting nuclei. Several studies^{2-6,13,21-23} have pointed out that the majority of the coincidence yield can be accounted for in terms of sequential decay of projectile-like and target-like fragments. As the bombarding energy increases, other non-sequential processes begin to compete in the production of light particles. The experimental challenge is to identify and separate these short and long decay processes in order to study the reaction mechanism.

The $^{16}\text{O}+\text{Ni}$ system and the similar system $^{16}\text{O}+\text{Ti}$ have been extensively studied.¹⁻⁶ Coincidence correlations of α particles and carbon ions have suggested the

presence of two nonsequential decay processes.^{2,4-6} The first component consists of α particles focused in the beam direction, having velocities similar to that of the beam and with an enhanced yield on the opposite side of the beam from the detected carbon ions. This component has been referred to as the fast or beam velocity component. The second component is characterized by α particles with velocities intermediate between the beam velocity and the velocity of the center of mass. The intermediate component has a maximum yield on the opposite side of the beam from the remnants of the projectile and in the general direction of the recoiling target nucleus. The energy spectra of α particles from the intermediate component are harder than expected from the equilibrated emission of the target nucleus as observed at backward angles. However, the spectra suggest a Coulomb barrier similar to that between the α particle and the target nucleus (TLF's).⁵

In this paper we report some results of an experiment designed to separate and better identify these two production sources of α particles in the peripheral collisions of 35 MeV/nucleon ^{16}O with $^{\text{nat}}\text{Ni}$. We find conclusive evidence that the fast component arises from the breakup of the projectile. Since this component cannot be accounted for by a sequential decay model, the time scale for the emission of these fast particles must be of the order of the collision time. We find that the source of the second intermediate component of α particles, also emitted nonsequentially, is identified to be the target nucleus.

We performed the experiment in the Michigan State University (MSU) 4π array,²⁴ using a beam of 35 MeV/nucleon ^{16}O ions accelerated by the K500 cyclotron at the National Superconducting Cyclotron Laboratory

to irradiate a nickel foil having a nominal thickness of 2.26 mg/cm^2 . Light charged particles and PLF's were detected in the forward array consisting of 45 fast/slow plastic scintillators covering an angular range between 7 and 18° with respect to the beam direction. Used in conjunction with the forward array, the MSU 4π array, consisting of fast/slow plastic scintillators, detected hydrogen and helium isotopes. The fast plastic ΔE scintillators had thicknesses of 1.6 mm and 3.2 mm in the forward array and the MSU 4π array, respectively. The forward array detectors had energy thresholds of 46 MeV and 260 MeV for α particles and carbon ions, respectively. The MSU 4π array had an α -particle energy threshold of 70 MeV .

In this paper, we focus on results of particle-particle correlations measured in the forward array using the $35 \text{ MeV/nucleon } ^{16}\text{O}$ projectiles. We refer to angles of the particle detectors on the same side of the beam as the detected PLF's with a positive sign and on the opposite side with a negative sign. The angles in this paper are given in spherical coordinates in the laboratory frame with the beam axis being the z axis.

In Figs. 1(a) and 1(b) for multiplicity=2 events in which two particles are detected and identified in the forward array, we present energy-energy correlations of α particles detected at the indicated angles in coincidence with carbon ions observed at $+10^\circ$. As we have seen before,^{5,6} we find the signature for sequential emission observed best on the same side [Fig. 1(a)] of the beam as the detected carbon ions. This signature is revealed by the pattern of two high-intensity regions with a pronounced valley in between them. On the opposite side of the beam in Fig. 1(b), the data show only one broad pattern consisting of α particles with an average velocity of 90% of the beam velocity and of carbon ions with an average velocity of 80% of the beam velocity. In Figs. 1(c) and 1(d), we show the projections of the yields onto the α -particle energy axis. The two lobes of Fig. 1(a) are seen as two bumps in Fig. 1(c). Sequential model calculations⁶ are shown as dashed curves (dim) for the sequential decay of TLF's, and dot-dashed curves for the sequential decay of the PLF's. The high-energy thresholds of the forward array prevent the observance of the sequential component from the TLF's. As a result most of the yield at $\theta_\alpha = +15^\circ$ is produced by the sequential breakup of ^{16}O . On the opposite side of the beam, the energy spectrum, shown in Fig. 1(d), is characterized by the large bump of α particles having 90% of the beam velocity. The fast component is manifested by this excess of high-energy α particles. The resulting fit by the model⁵ of this component is shown as a dotted curve. From previous studies,^{2,5} we expect that at energies lower than 100 MeV , the spectrum also indicates an excess in the yield of α particles that cannot be accounted for in terms of the sequential emission from PLF's and TLF's. This excess at intermediate energies, shown in Figs. 1(c) and 1(d) by the bold dashed curve, reflects the presence of the intermediate component of nonsequentially emitted α particles.⁵

In order to understand better the binary nature of breakup of the projectile, we examine the correlation of atomic numbers from multiplicity=2 events. Figures 2(a) and 2(b) presents ions of atomic number Z_2 detected between $\theta_{Z_2} = \pm(7^\circ \rightarrow 18^\circ)$ on the same side [Fig. 2(a)] and opposite side [Fig. 2(b)] of the beam from Z_1 detected at $\theta_{Z_1} = +10^\circ$. As can be seen along the solid line of $Z_1 + Z_2 = 8$, the $^{12}\text{C} + \alpha$ channel is the most probable two-body decay mode of ^{16}O on both sides of the beam. There may be a substantial number of events for the proton pickup channel, $Z_1 + Z_2 = 9$ (dashed line), but many fewer for the α -particle pickup channel, $Z_1 + Z_2 = 10$ (dot-dashed line). The distributions in this figure along

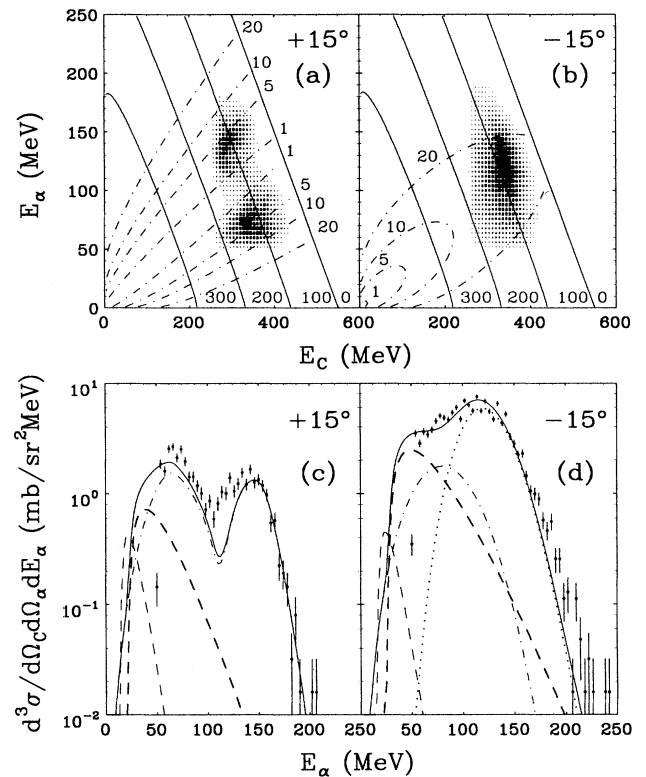


FIG. 1. Density plots [(a) and (b)], with the intensity varying linearly, for α particles at the indicated angles in coincidence with carbon at $\theta_C = +10^\circ$. The data have been smoothed using a two-dimensional Gaussian distribution, and gray scaled with 8×8 pixel cells. Curves represent three body kinematic calculations. The dot-dashed curves correspond various values of the relative energy (MeV) between ^{12}C and α particle assuming the breakup of ^{16}O into $^{12}\text{C} + \alpha$. The solid curves correspond to the total excitation energy, Q_3 (MeV). (d) and (c) show the projections onto the energy axis of the α particles with dashed (dim), and dot-dashed curves representing the calculated contributions from the sequential decay of TLF's and PLF's, respectively. The contributions of the intermediate and fast components are represented by calculated dashed (bold) and dotted curves, respectively. The solid curve represents the sum of the contributions from the fast, intermediate components and the sequential decay of the PLF's.

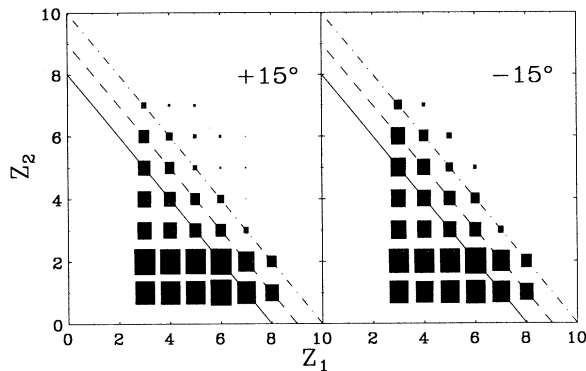


FIG. 2. Coincidences between ions of atomic number Z_2 observed on the opposite side of the beam from the detected Z_1 . Solid, dashed, and dotted lines indicate events in which the sum of $Z_1 + Z_2$ is equal to the atomic number of the projectile, Z_{PRO} , is equal to $Z_{\text{PRO}} + 1$ and is equal to $Z_{\text{PRO}} + 2$, respectively. The intensity scale reflects the logarithm of the counts.

the $Z_1 + Z_2$ lines suggest that most of these fragments come from the projectile breakup. Fragments whose sum of atomic numbers is less than the atomic number of the projectile may result from the multiple decay of highly excited states of the projectile.

To test the hypothesis of the multiple breakup of the projectile, we consider multiplicity=3 events in the forward detector array in which Z_1 and Z_3 are detected on the same side of the beam. We define the xz plane by the direction of Z_1 and the beam axis, i.e., $\phi_1 = 0^\circ$. For particles with Z_2 detected on the opposite side of the beam from Z_1 we have selected ϕ_2 to be between 160 and 200° . Correlations between the atomic numbers of Z_1 and Z_2 on the opposite side of the beam each other are shown in Fig. 3 with the third fragment, Z_3 , indicated in the figure. Since the distributions of products are limited by the solid line of $Z_1 + Z_2 + Z_3 = 8$ as in the case of multiplicity=2 events, the majority of the yield can be understood in terms of the multiple decay of the excited projectile. Such correlations of atomic numbers of products observed on the opposite sides of the beam suggest that most of the light particles emitted on the opposite side of the beam from the observed PLF's may indeed have their origin in the projectile.

In order to identify clearly the source of the fast component of α particles shown in Figs. 1(b) and 1(d), we reconstruct the projectile by detecting an α particle in the vicinity of a ^{12}C on the same side of the beam. We are confident that the projectile can be reconstructed because of the following reasons. First, from Figs. 1(a) and 1(c), we can see that the majority of the α - ^{12}C yield at $\theta_\alpha = +15^\circ$ results from the breakup of ^{16}O . Secondly, with the large energy thresholds, the contribution from the decay of TLF's as seen by the forward array is of the order of a few percent. Thirdly, since the α -particle pickup channel is weak, we do not expect that the C- α - α events arise from the double α -particle decay of ^{20}Ne . By detecting an α particle on the same side of the beam as

the ^{12}C , the data indicate that we can, with a high probability, reconstruct the projectile. In coincidence with the reconstructed projectile we select multiplicity=3 events in which three particles are detected and identified in the forward array, where a second α particle appears on the opposite side of the beam from the reconstructed projectile. In Fig. 4(a) we represent by open circles the energy spectrum of the second α particle on the opposite side of the beam. In order to compare the shape of this spectrum with that of multiplicity=2 events, the energy spectrum of α particles, shown previously in Fig. 1(d), is presented in Fig. 4(a) as a histogram. As mentioned above, the fast component is manifested by the presence of the high-energy bump in the histograms in Fig. 4. Since in the case of C- α - α events the projectile has been reconstructed, these α particles on the opposite side of the beam from the reconstructed projectile can only come from the target nucleus. The absence of the high-energy bump in the α -particle energy spectrum of C- α - α multiplicity=3 events (open circles) indicates conclusively that the fast, beam velocity component of α particles arises from the breakup of the projectile.

In the case of ^{12}C - p - α events [solid circles in Fig. 4(a)] in which a proton is detected on the same side of the beam as the carbon ions, the proton may come from the

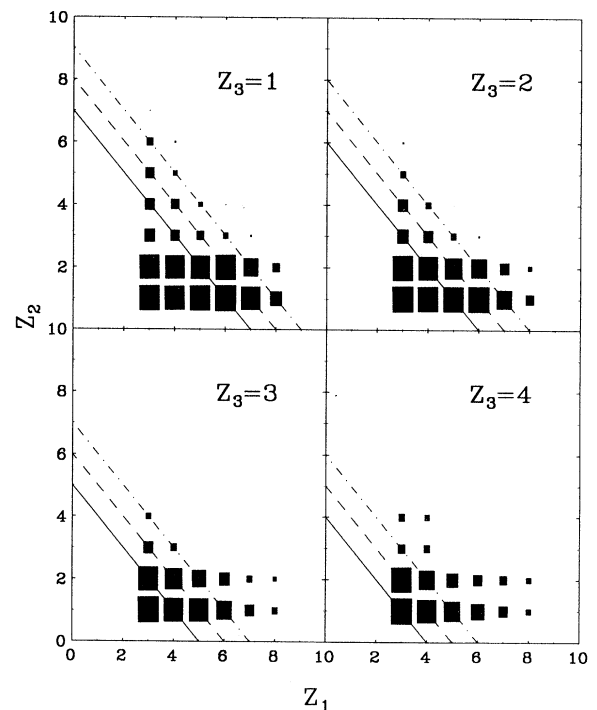


FIG. 3. Triple coincidences among ions of atomic number Z_2 observed on the opposite side of the beam from the detected Z_1 and Z_3 . Solid, dashed, and dotted lines indicate events in which the sum of $Z_1 + Z_2 + Z_3$ is equal to the atomic number of the projectile, Z_{PRO} , is equal to $Z_{\text{PRO}} + 1$ and is equal to $Z_{\text{PRO}} + 2$, respectively. The intensity scale reflects the logarithm of the counts.

projectile (proton pickup) or from the target nucleus. In either case, the α particle will come mostly from the breakup of the projectile. The energy spectrum of the α particle on the opposite side of the beam shown in Fig. 4(a) for the C- p - α events is very similar to the energy spectrum (histogram) from C- α multiplicity=2 events, thus confirming that the high-energy α particles come from the breakup of the projectile. In Fig. 4(b), we also present the α -particle energy spectra (solid circles) for the B- α - α , Be- α - α , and Li- α - α multiplicity=3 events. These triple coincidence energy spectra are compared to the double coincidence energy spectra for α particles in coincidence with B, Be, and Li ions (histograms). The B- α - α events select the proton pickup channel, whereas, the Be- α - α and Li- α - α events result from the direct, multiple decay of the projectile without the necessity of picking up nucleons from the target. These triple coincidence energy spectra have the same shape as the spectra for the mul-

tiplicity=2 events, indicating that the fast component of nonsequentially emitted α particles is a general feature of the decay mode of the projectile. Since it has been established that the fast component is a result of the breakup of the projectile, the presence of the fast component in these triple coincidence energy spectra strongly suggests that the projectile undergoes multiple α -particle decay, leading to the production of multiple energetic light particles. These studies provide conclusive evidence that the projectile is the source of the fast, beam velocity component focused on the opposite side of the beam from the detected PLF's.

The model calculation describes very well the sequential decay characteristics reflected by the shape and magnitude of the energy spectrum of α particles observed on the same side of the beam as the detected carbon ions, shown above in Fig. 1(c). At these coincidence angle pairs where sequential decay processes are separated most clearly, we fix the parameters in the model associated with the excitation energy distribution and energy and angular distributions of the primary ^{16}O prior to decay. With this set of parameters that best describe the data on the same side of the beam, we are unable to describe the energy spectrum of the fast component, shown above in Fig. 1(d), of α particles detected on the opposite side of the beam. Even though the fast, beam velocity component has its origin in the projectile, such α particles do not come from sequential emission processes and so must be emitted on a time scale shorter than the time scale for sequential emission.

The narrow dashed (dim) curve in Fig. 4(a) represents the calculated energy spectrum of α particles emitted sequentially by TLF's in coincidence with carbon ions. These calculations are based on the α -particle energy spectra observed at backward angles.⁵ For C- α - α events, the energy spectrum of α particles on the opposite side of the beam from the observed carbon ions, that must come from the TLF's, is much harder than the expected spectrum for α particles emitted sequentially by the TLF's, but is similar to the spectrum expected for the intermediate component shown by the broad dashed (bold) curve.⁵ The absence of the high-energy bump in the α -particle energy spectrum for the C- α - α events [open circles in Fig. 4(a)] also indicates that the α -particle pickup channel, and subsequent double α -particle decay from ^{20}Ne , is not contributing to these events. If the C- α - α events resulted from this process, then the α -particle energy spectrum should look like the spectra for the cases of B- α - α , Be- α - α , and Li- α - α in Fig. 4(b) where multiple decay of the projectile seems to explain the data. Therefore, the triple coincidence correlations suggest that the TLF's are the source of the intermediate component of α particles. Since for these events the projectile is reconstructed, it cannot be the source. Because the intermediate component of α particles cannot be accounted for in terms of sequential decay processes, it must be produced during the early stages of the collision.

In conclusion, we find that triple coincidence correla-

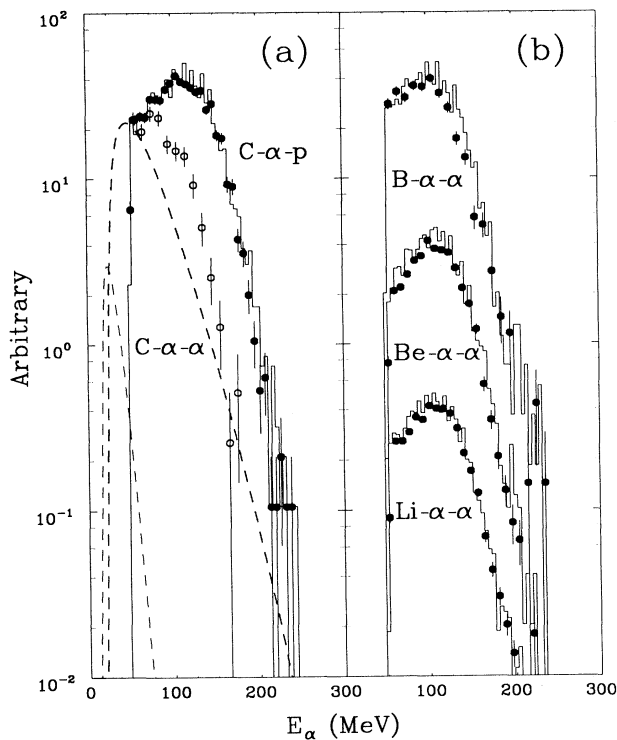


FIG. 4. Energy spectrum of α particles [histogram in (a)] in coincidence with carbon ions detected on the opposite side of the beam (double coincidences). Open circles (a) represent the energy spectrum of α particles detected on the opposite side of the beam from the reconstructed ^{16}O (triple coincidences). Solid circles (a) represent C- p - α triple coincidence events. Narrow dashed (dim) and the broad dashed (bold) curves represent the calculated contribution from the sequential decay of TLF's and the intermediate component. Similarly, data are shown as solid circles in (b) for B- α - α , Be- α - α , and Li- α - α triple coincidences. Energy spectra of α particles [histograms in (b)] in coincidence (double) with B, Be, and Li ions detected on the opposite side of the beam.

tions between the reconstructed projectile and an α particle detected on the opposite side of the beam from the detected ^{12}C conclusively reveal that the fast, beam velocity component of α particles previously observed in coincidence with projectile-like fragments arises from the breakup of the projectile. In addition, the correlations seem to indicate that the target nucleus is the origin of the intermediate component of α particles. Both of these

components are produced by mechanisms leading to the emission of α particles during the early stages of the collision.

We wish to acknowledge the support of the operations crew of the National Superconducting Cyclotron Laboratory. This research was supported by the National Science Foundation under Grants Nos. PHY-8611210 and PHY-8708093.

-
- *Permanent address: University of Michigan, 4901 Evergreen Road, Dearborn, MI 48128.
- ¹H. Ho, R. Albrecht, W. Dünneweber, G. Graw, S.G. Steadman, J.P. Wurm, D. Disdier, V. Rauch, and F. Scheibling, *Z. Phys. A* **283**, 235 (1977).
 - ²H. Ho, P. Gonthier, M.N. Namboodiri, J.B. Natowitz, L. Adler, S. Simon, K. Hagel, R. Terry, and A. Khodai, *Phys. Lett.* **96B**, 51 (1980).
 - ³H. Ho, P.L. Gonthier, G.-Y. Fan, W. Kühn, A. Pfoh, L. Schad, R. Wolski, J.P. Wurm, J.C. Adloff, D. Disdier, A. Kamili, V. Rauch, G. Rudolf, F. Scheibling, and A. Strazzeri, *Phys. Rev. C* **27**, 584 (1983).
 - ⁴P.L. Gonthier, H. Ho, N.M. Namboodiri, J.B. Natowitz, L. Adler, S. Simon, K. Hagel, S. Kniffen, and A. Khodai, *Nucl. Phys. A* **411**, 289 (1983).
 - ⁵P.L. Gonthier, B. Bouma, P. Harper, R. Ramaker, D.A. Cebra, Z.M. Koenig, D. Fox, and G.D. Westfall, *Phys. Rev. C* **35**, 1946 (1987).
 - ⁶P.L. Gonthier, P. Harper, B. Bouma, R. Ramaker, D.A. Cebra, Z.M. Koenig, D. Fox, and G.D. Westfall, *Phys. Rev. C* **41**, 2635 (1990).
 - ⁷P.A. Gottschalk and M. Weström, *Nucl. Phys. A* **314**, 232 (1979).
 - ⁸J.P. Bondorf, J.N. De, G. Fáí, A.O.T. Karvinen, B. Jakobsson, and J. Randrup, *Nucl. Phys. A* **333**, 285 (1980); M.C. Robel, Ph. D. thesis, Lawrence Berkeley Laboratory Report No. LBL-8181, 1979.
 - ⁹D.H.E. Gross and J. Wilczyński, *Phys. Lett.* **67B**, 1 (1977).
 - ¹⁰R.K. Bhowmik, E.C. Pollacco, N.E. Sanderson, J.B.A. England, and G.C. Morrison, *Phys. Rev. Lett.* **43**, 619 (1979).
 - ¹¹R. Billerey, C. Cerruti, A. Chevarier, N. Chevarier, B. Cheynis, and A. Demeyer, *Z. Phys. A* **292**, 293 (1979).
 - ¹²A. Gamp, J.C. Jacmart, N. Poffé, H. Doubre, J.C. Roynette, and J. Wilczynski, *Phys. Lett.* **74B**, 215 (1978).
 - ¹³J. van Driel, S. Gonggrijp, R.V.F. Janssens, R.H. Siemssen, K. Siwek-Wilczynska, and J. Wilczynski, *Phys. Lett.* **98B**, 351 (1981).
 - ¹⁴W.D. Rae, A.J. Cole, A. Dacal, R. Legrain, B.G. Harvey, J. Mahoney, M.J. Murphy, R.G. Stokstad, and I. Tserruya, *Phys. Lett.* **105B**, 417 (1981).
 - ¹⁵W. Terlau, M. Bürgel, A. Budzanowski, H. Fuchs, H. Homeyer, G. Röschert, J. Uckert, and R. Vogel, *Z. Phys. A* **330**, 303 (1988).
 - ¹⁶M.B. Tsang, W.G. Lynch, R.J. Puigh, R. Vandenbosch, and A. G. Seamster, *Phys. Rev. C* **23**, 1560 (1981).
 - ¹⁷R. K. Bhowmik, J. van Driel, R.H. Siemssen, G.J. Balster, P.B. Goldhoorn, S. Gonggrijp, Y. Iwasaki, R.V.F. Janssens, H. Sakai, K. Siwek-Wilczynska, W.A. Sterrenburg, and J. Wilczynski, *Nucl. Phys. A* **390**, 117 (1982).
 - ¹⁸H. Homeyer, M. Bürgel, M. Clover, Ch. Egelhaaf, H. Fuchs, A. Gamp, D. Kovar, and W. Rauch, *Phys. Rev. C* **26**, 1335 (1982).
 - ¹⁹E. Takada, T. Shimoda, N. Takahashi, T. Yamaya, K. Nagatani, T. Udagawa, and T. Tamura, *Phys. Rev. C* **23**, 772 (1981).
 - ²⁰T. Fukuda, M. Ishihara, M. Tanaka, I. Miura, H. Ogata, and H. Kamitsubo, *Phys. Rev. C* **25**, 2464 (1982).
 - ²¹G.R. Young, R.L. Ferguson, A. Gavron, D.C. Hensley, Felix E. Obenshain, F. Plasil, A.H. Snell, M.P. Webb, C.F. Maguire, and G.A. Petitt, *Phys. Rev. Lett.* **45**, 1389 (1980).
 - ²²H. Gemmeke, P. Netter, Ax. Richter, L. Lassen, S. Lewandowski, W. Lücking, and R. Schreck, *Phys. Lett.* **97B**, 213 (1980).
 - ²³M. Bini, C.K. Gelbke, D.K. Scott, T.J.M. Symons, P. Doll, D.L. Hendrie, J.L. Laville, J. Mahoney, M.C. Mermaz, C. Olmer, K. Van Bibber, and H.H. Wieman, *Phys. Rev. C* **22**, 1945 (1980).
 - ²⁴G.D. Westfall, J.E. Yurkon, J. Van der Plicht, Z.M. Koenig, B.V. Jacak, R. Fox, G.M. Crawley, M.R. Maier, and B.E. Hasselquist, *Nucl. Instrum. Methods A* **238**, 347 (1985).